Materiales de Construcción 75 (358)
April-June 2025, e370
ISSN-L: 0465-2746, eISSN: 1988-3226
https://doi.org/10.3989/mc.2025.387824

Effect mechanism of particle size and interface geometry characteristics on shear mechanical behavior of sand-concrete interface

Z. Meng[a], Y. Li[b], H. Li[a] ✉, J. Xu[b], S. Shen[c]

a. School of Civil Engineering and Architecture, NingboTech University, (Ningbo, China)
b. School of Civil Engineering, Anhui Jianzhu University, (Hefei, China)
c. China MCC22 Group Corporation Ltd., (Tangshan, China)
✉: huanhuanli17@nbt.edu.cn

Received 13 June 2024
Accepted 10 October 2024
Available on line 27 August 2025

ABSTRACT: The effects of sand grain size and interface groove spacing on the shear behavior of the sand-concrete interface were investigated under consistent roughness conditions through a series of interface shear tests. Tests utilized different grain sizes of sand and concrete slabs with varying surface textures, based on the sand pouring method. The results were compared with those of pure sand shear tests to evaluate variation characteristics in parameters such as shear stress and friction angle in the interface shear tests. Additionally, the particle flow model was employed to comprehensively analyze rotation characteristics of sand particles and the development trend of shear band width. The findings indicate that: (1) interface shear strength is closely linked to grain size distribution range and groove spacing; (2) thickness of the shear band is positively correlated with particle size, while its correlation with groove spacing is weaker.

KEYWORDS: Sand-concrete contact surface; Contact surface roughness; PFC particle flow program; Semicircular groove texture; Sand particle size range.

Citation/Citar como: Meng Z, Li Y, Li H, Xu J, Shen S. 2025. Effect mechanism of particle size and interface geometry characteristics on shear mechanical behavior of sand-concrete interface. Mater. Construcc. 75(358):e370. https://doi.org/10.3989/mc.2025.387824

RESUMEN: *Mecanismo de influencia del tamaño de las partículas y las características geométricas de la interfaz en el comportamiento mecánico de corte de la interfase arena-hormigón.* Para estudiar el efecto del tamaño de grano de arena y el espaciado de ranuras en el corte de la interfase arena-hormigón, se realizaron ensayos usando el método de irrigación de arena. Se usaron arenas de diversos tamaños y losas de hormigón con diferentes texturas superficiales. Se analizaron cambios en el esfuerzo cortante y el ángulo de fricción. También, se empleó un modelo de flujo de partículas para examinar cómo las características de rotación de las partículas de arena influyen en el ancho de la banda de corte. Los resultados mostraron que: (1) La resistencia al corte de la interfaz está estrechamente relacionada con la distribución del tamaño de las partículas y el espaciado de las ranuras; (2) El grosor de la banda de corte se correlaciona positivamente con el tamaño de las partículas, mientras que su relación con el espaciado de las ranuras es menos notable.

PALABRAS CLAVE: Superficie de contacto arena-hormigón; Rugosidad; Programa de Flujo de Partículas PFC; Textura de ranura semicircular; Gama granulométrica de la arena.

1. INTRODUCTION

Soil-artificial structure contact surfaces widely exist in geotechnical infrastructure, such as pipelines, retaining walls, anchors, pile foundations, abutments, slopes, and various other geotechnical structures (1-3). The shear strength of the contact surface is frequently lower than that of the soil's interior, rendering the contact surface vulnerable as the primary point of instability in geotechnical engineering. Investigating the interaction mechanisms between soil particles and the concrete interface, as well as enhancing the interface shear strength, is crucial for improving the safety of geotechnical engineering. The interfacial interaction mechanism primarily relies on the soil material, the surface properties of the artificial structure, and the pressure conditions. Key factors influencing the soil material include porosity, particle size distribution, particle shape, compactness, particle stiffness, and drainage conditions (4-10) and significant factors influencing the surface properties of the structure encompass surface roughness, surface stiffness, and texture arrangement characteristics(11-14).

Macroscopic factors such as porosity, compactness, and drainage conditions are easily measurable in laboratory, and the influence of macroscopic factors on interface shear strength is already clear, while the impact of microscopic factors like particle size range, shape, particle stiffness, surface roughness, and other variables on interface shear strength remains under-researched (15). Research had demonstrated that the peak shear strength of the interface exhibited a significant positive correlation with changes in coarse particle content and particle size ratio. However, this correlation diminished as the coarse particle content increases beyond a certain threshold. Conversely, the residual shear strength showed a negative correlation with coarse particle content (16). The thickness of the interface shear band showed a correlation with the coarse particle content in stages. Specifically, when the coarse particle content was low, the two were positively correlated, but when the content exceeded a certain proportion, they became negatively correlated (17). Because of the inherent randomness and complexity of soil particles, the research on particle size distribution, particle shape and other microscopic influencing factors were still at the stage of phenomenal analysis. A unified system of quantitative indexes for microscopic parameters of particles had not yet been established (18, 19). Furthermore, numerous studies had improved surface roughness by incorporating regular or irregular texture patterns onto structural surfaces, resulting in a notable increase in interface shear strength. The extent of enhancement in shear strength was closely related to factors such as the form, geometric characteristics, and spatial distribution of the pattern (20, 21).

Currently, the direct shear test remains the most prevalent and stable method compared to other interface test methods (such as tilt table test, ring shear test). It had been extensively used to investigate the shear behavior of soil-geotechnical material interfaces, soil-steel material interfaces, and soil-concrete interfaces (22-27). It was worth noting the rapid development in test materials and observation methods, such as Particle Image Velocimetry (PIV), soil particle 3D printing technology, Computed Tomography, particle stiffness measurement technology, and transparent soil technology (28-30), these advancements had enabled the analysis of interfacial shear mechanisms at the mesoscopic scale. Furthermore, with the advancement of numerical simulation technology, the Discrete Element Method (DEM), which involved generating soil particles and assembling them into geological bodies, had been extensively utilized (31-36), this method could realize the large-scale interactions between particles and particles and between particles and structures, allowing the assembly of spherical particles into new particles with complex morphology. Consequently, it offered an effective analytical tool for uncovering the mechanism of particle combination on the overall behavior of the soil. Currently, microscopic parameters are typically calibrated through macroscopic phenomena, such as particle stiffness, particle friction coefficient, particle elastic modulus, and other parameters, directly establishing particle mesoscopic parameters through indoor experiments remains challenging (37, 38).

In summary, extensive research had delved into various factors such as different material structures, surface roughness, surface texture pattern types, coarse particle content, particle shape, and others. These studies had led to significant progress in understanding interface shear behavior. However, research on the interfacial shear behavior of concrete surfaces with different morphological characteristics and particle size ranges under the same roughness conditions is relatively scarce. In this study, concrete slabs with different semi-circular groove spacings were designed using the sand filling method while maintaining the same surface roughness. Additionally, three types of sand materials with typical particle size ranges were prepared (Type A sand (0.075-0.5 mm), Type B sand (0.5-2 mm), and Type C sand (2-5 mm)). To avoid the influence of particle shape, the three types of sand were sourced from the same location and possessed identical particle strength conditions and shape characteristics. Through standard direct shear tests, shear displacement-stress curves were obtained for both pure sand and sand-concrete interfaces with varying particle size ranges. Furthermore, a numerical model under identical conditions was established using Discrete Element Method (DEM) for comprehensive analysis. The influence of sand particle size range and groove arrangement characteristics on interface shear strength was analyzed. In this study, it was found that different morphological characteristics and different particle size ranges did have a significant effect on the shear behavior of the interface. The results of the study revealed the influencing mechanism of particle size and geometric characteristics of the interface on the shear mechanical behavior of the sand-concrete interface, and it was found that the shear strength could be increased by up to 29.3% by adjusting the groove morphology. The results of the research could be widely used in actual projects such as retaining walls, pile foundations and underground structures. Engineers could choose the appropriate design scheme of the interface according to the characteristics of sand materials at different sites to improve the stability and bearing capacity of engineering structures. The data of the thickness of shear band and shear strength obtained in the study could be used to validate and calibrate the numerical model under similar working conditions, thus improving the accuracy of the prediction of engineering behavior under complex geological conditions.

2. TEST METHOD AND MATERIAL

2.1. Preparation of test samples

To investigate the variations in interface shear strength under different particle sizes and numbers of grooves, three types of natural sand with distinct particle size ranges were screened: Type A sand (2-5mm), Type B sand (0.5~2mm), and Type C sand (0.075~0.5mm). The basic physical parameters of the sand materials were outlined in Table 1, the sand samples were shown in Figure 1, and the sand gradation curve was presented in Figure 2. The test equipment utilized was the ZJ type strain-controlled direct shear instrument manufactured by Nanjing Soil Instrument Factory Co., Ltd.

Figure 1. The appearance of particles in three types of sand samples.

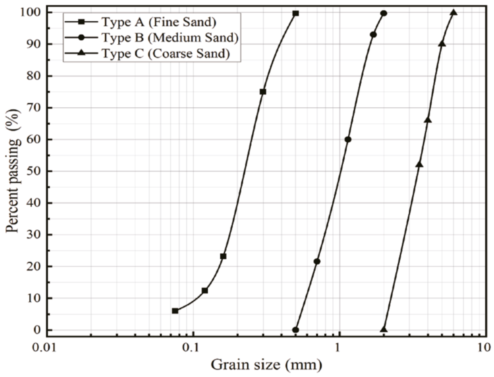

Figure 2. Particle size of all three sands used in this study.

Table 1. The physical properties indicators of three types of sand soil samples.

Physical properties indicators	Coarse sand (Type A)	Medium sand (Type B)	Fine sand (Type C)
D_{10}	2.24	0.59	0.1
D_{30}	2.81	0.78	0.178
D_{50}	3.47	1.0	0.22
D_{60}	3.8	1.15	0.25
Coefficient of uniformity (Cu)	1.70	1.95	2.50
Coefficient of curvature (Cc)	0.93	0.90	1.27
*D*r (%)	50	50	50
ρ_{min} (g/cm^3)	1.25	1.30	1.33
ρ_{max} (g/cm^3)	1.70	1.61	1.58
Maximum void ratio (e_{max})	1.14	1.03	0.97
Maximum void ratio (e_{min})	0.57	0.64	0.66
void ratio (e_0)	0.86	0.84	0.82
Particle specific gravity (G_s)	2.67	2.64	2.62
V (cm^3)	60	60	60
m_s (g)	85.7	86.1	86.4
m_w (g)	16.7	16.4	16.2

Before conducting the test, a self-made glass mold was used to carry out concrete mud diffusion test based on sand filling method, and a random sand-concrete interface was prepared under the action of gravity. Based on CT technology, Ms voxel 450 industrial CT scanner was used to scan the test sample, and 9 slice images of the 3D model of mud diffusion samples were obtained to determine the average sand filling depth of the grooves on the concrete surface (39). The contact cross-section curve was considered as a function of x, with the lowest point of the contact surface designated as the y=0 position, as shown in Figure 3. The average depth of sand filling was obtained by integrating according to Equation [1], which was the average surface roughness (Ra), and the random surface morphology roughness of concrete measured in this study was 2.64 mm.

$$R_a = \frac{1}{L}\int_0^L |Y(x)|\,dx \qquad [1]$$

Where R_a is the average surface roughness, L is the sampling length, Y is the height of the contact surface, and x is the distance of the contact surface from the left endpoint.

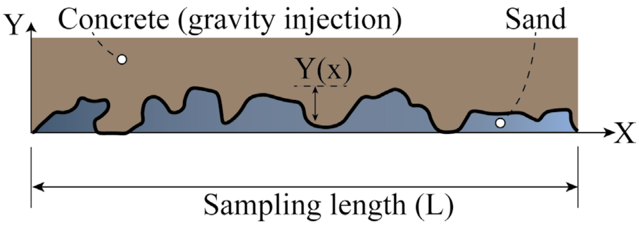

Figure 3. Schematic diagram of surface roughness function.

The groove-like contact form was indeed one of the more common random contact forms. In this study, the random groove form was generalized into an ideal semicircular groove, and the impact of the number of grooves on the interface shear behavior under the same roughness condition was studied. In order to maintain the same roughness as the natural concrete interface, three types of concrete specimens with the same roughness as the random surface were prepared in this study by varying the groove spacing and groove radius, and the number of grooves was n=5/9/ 13 respectively. The dimensions of concrete specimens with different number of grooves were shown in Table 2 and the morphology of concrete specimens with different number of grooves was shown in Figure 4. The concrete was poured into the molds and demoulded to obtain the grooved concrete specimens used in the test, which was composed of water, cement, sand and stone, and the mix ratio of the concrete material was 0.5:1:2.11:2.53. The molds were prepared by 3D printing technology. Firstly, the 3D models of the concrete block test molds were drawn by SolidWork software, and then the linear resin material was heated and extrated by the processing head of the 3D printer to produce the concrete block test molds with different contact surface shapes, as shown in Figure 5. concrete block test molds. The concrete was poured into the molds and then demolded to obtain the grooved concrete specimens used in the test, as shown in Figure 6.

Table 2. Design parameters of concrete test blocks with different numbers of grooves.

Concrete test block	L (mm)	H (mm)	l_1 (mm)	l_2 (mm)	l_3 (mm)	h_1 (mm)
n=5	96	20	10.92	5.9	8.9	5.46
n=9	96	20	8.14	1.67	4.69	4.07
n=13	96	20	6.78	0.13	3.15	3.39

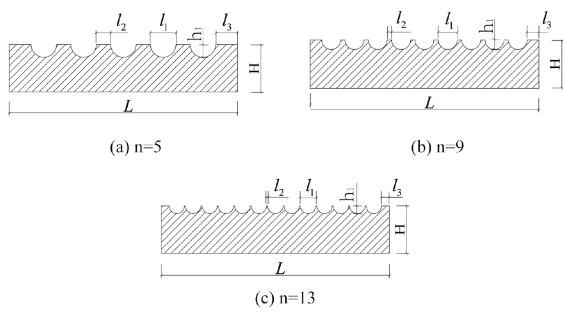

Figure 4. Geometric characteristics of semicircular contact surfaces with different number of grooves.

Figure 5. Concrete block test molds.

Figure 6. Concrete specimens used in the test.

2.2. Test plan

To investigate the influence of different numbers of semicircular grooves and varying sand particle size ranges on the shear mechanical properties of the contact surface under the same roughness (2.6mm), direct shear tests were conducted on the three types of configured sand according to the test scheme combinations outlined in Table 3. The vertical pressures at all levels in the direct shear test should be applied according to the engineering reality and the softness or hardness of the soil, the difference between the vertical pressures at all levels should be roughly equal. In the actual operation process, considering the characteristics of the sand sample and the function of the physical experiment device, in order to prevent the crushing of the sand particles when they passed over the grooves due to excessive pressure, the normal stress was determined as 50kPa, 100kPa, 200kPa, 300kPa. The principle of the direct shear test at the semicircular groove interface was shown in Figure 7.

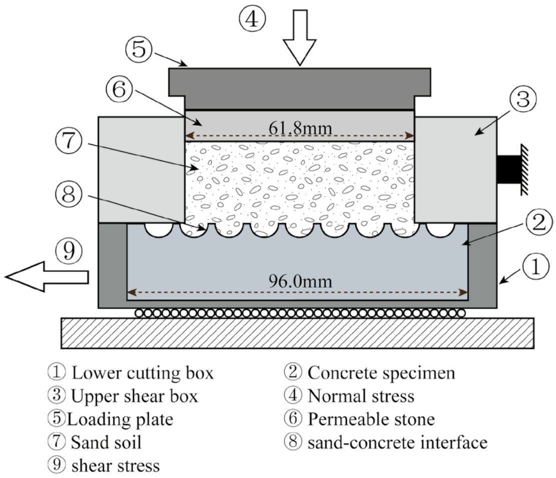

Figure 7. Principle of semicircular groove interface direct shear test.

Table 3. Direct shear test scheme.

Sandy soil type	Number of grooves		
	5	9	13
Type A	A5	A9	A13
Type B	B5	B9	B13
Type C	C5	C9	C13

3. TEST RESULTS AND ANALYSIS

3.1. Analysis of shear stress-displacement curves

Figure 8 to Figure 10 shower the shear stress-shear displacement relationship curves of three types of sand at the interface with varying numbers of grooves under different normal stresses. In the case of the same roughness of the contact surface, it could be seen that when the sand particle size range was smaller, the trend of the curve was gentler, the process of reaching shear failure stress was more uniform, and there were fewer protruding points on the curve. It was due to the fact that during the shear test, the smaller the particle size of the sand, the smoother it passed through the grooves on the surface, and the less resistance it had to friction with the surrounding collision.

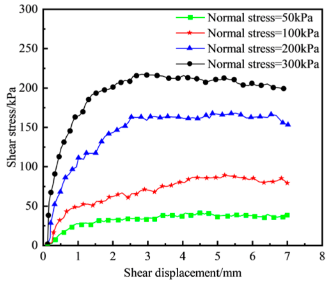

(a) n=5

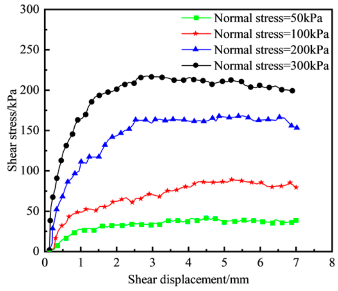

(b) n=9

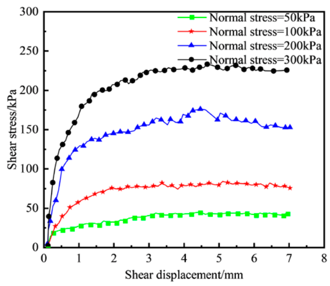

(c) n=13

FIGURE 8. Shear stress-shear displacement curves of Type A sandy soil under different normal stresses and groove numbers.

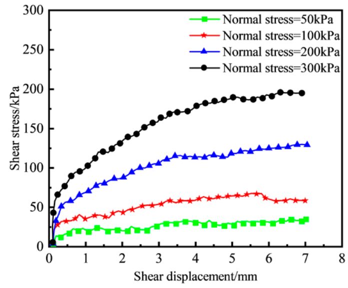

(a) n=5

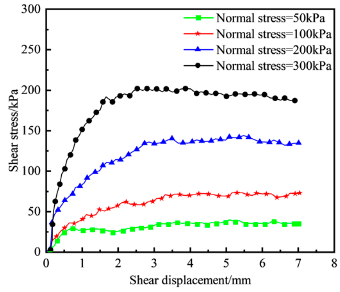

(b) n=9

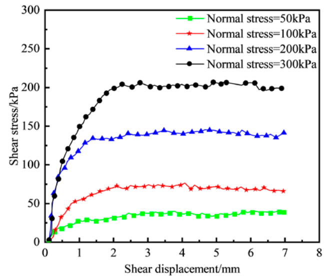

(c) n=13

FIGURE 9. Shear stress-shear displacement curves of Type B sandy soil under different normal stresses and groove number.

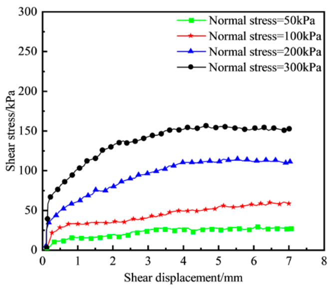

(a) n=5

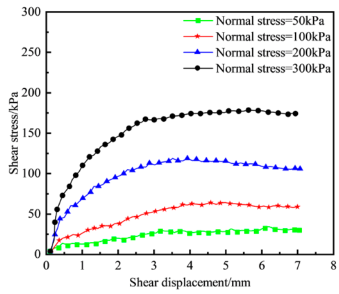

(b) n=9

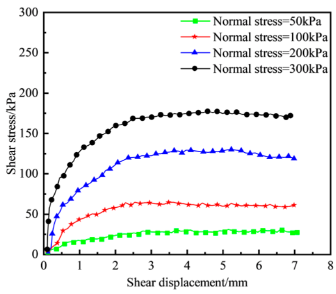

(c) n=13

FIGURE 10. Shear stress-shear displacement curves of Type C sandy soil under different normal stresses and groove numbers.

3.2. Shear strength of contact surface and internal friction angle

Four kinds of vertical load σ used in the test were 50 kPa, 100 kPa, 200 kPa, and 300 kPa, and the shear strength τf corresponding to each level of vertical load could be obtained at the end of the test. According to the Mohr-Coulomb strength theory, the formula for the shear strength in the direct shear test is τf = cf +σtanφ. The cohesive strength and friction coefficient were obtained by fitting the data with OriginPro 2024 (64-bit) SR1 software, and the results are shown in Table 5.

Taking the shear strength under 300kPa normal stress as an example, the direct shear strengths of different types of sand at surfaces with different numbers of grooves were shown in Table 4. When the number of grooves in the concrete test block was 5, the shear strength of Type A sand was 9.93% higher than that of Type B sand and 25.16% higher than that of Type C sand. When the number of grooves in the concrete test block was 9, the shear strength of Type A sand was 7.68% higher than that of Type B sand and 25.68% higher than that of Type C sand. When the number of grooves in the concrete test block was 13, the shear strength of Type A sand was 11.06% higher than that of Type B sand and 31.08% higher than that of Type C sand. The shear strength fitting equation and parameters of the interface between sand and concrete slabs were shown in Table 5. From the table, the cohesion and internal friction angle of sand in different particle size ranges and the correlation coefficients of the fitting equation could be visually compared.

Table 4. Shear strength between different sand soil types and different numbers of grooves (under 300kPa normal stress).

Sandy soil type	Number of grooves		
	5	9	13
Type A	190.15	217.23	228.46
Type B	172.98	201.73	205.71
Type C	151.92	201.73	174.29

Table 5. Fitting equations and parameters of shear strength for different sands and different grooved concrete contact surfaces.

Number of grooves	Particle size ranges (mm)	Curve equations	c_f (kPa)	φ (°)	R^2
n=5	Type A sand	τ_f=0.9536+0.6345σ	0.9536	32.40	0.999
	Type B sand	τ_f=0.4307+0.5738σ	0.4307	29.85	0.999
	Type C sand	τ_f=0.2497+0.5157σ	0.2497	27.28	0.997
n=9	Type A sand	τ_f=0.9536+0.7512σ	0.9536	36.91	0.996
	Type B sand	τ_f=0.4307+0.6811σ	0.4307	34.26	0.999
	Type C sand	τ_f=0.2497+0.5809σ	0.2497	30.15	0.997
n=13	Type A sand	τ_f=0.9536+0.7855σ	0.9536	38.15	0.997
	Type B sand	τ_f=0.4307+0.6977σ	0.4307	34.90	0.999
	Type C sand	τ_f=0.2497+0.6012σ	0.2497	31.01	0.996

In order to investigate the effects of changes in grain size and the number of grooves on the peak shear strength of the interface, the median particle size (D50), which is a measure of the change in particle size of the sand, and the number of grooves, which characterizes the change in the morphology of the contact surfaces, were used as variables, and the peak shear strength of the interface was used as the dependent variable. In this study, the Origin Pro 2024 (64-bit) SR1 software was used to fit the data into mathematical equations, and various fitting modes, such as linear fitting, polynomial fitting, and nonlinear curve fitting, were attempted. In the process of fitting the particle size (D50) to the peak shear strength of the interface as a function, when the 'Quick Fit' category included in nonlinear curve fitting was tried, the Logistic function contained in 'Quick Fit' met the requirements, and the basic format of the function was:

$$y = \frac{A_1 - A_2}{1 + (x / x_0)^p} + A_2 \qquad [2]$$

During fitting, the Levenberg-Marquardt iterative algorithm was used to gradually approximate the original data, the fitting curves obtained were shown in Figure 11, and the fitting functions obtained were shown in Table 6. As the coefficient of determination R2 varied from 0.99885 to 0.99897, the fitting accuracy met the requirements. In the process of fitting the number of grooves to the peak shear strength of the interface as a function, the nonlinear curve fitting was also used, when the 'Origin Basic Functions' category was used, the 'ExpAssoc' function contained in 'Origin Basic Functions' met the requirements, and the basic format of the function was:

$$y = y_0 + A_1(1 - e^{-x/t_1}) + A_2(1 - e^{-x/t_2}) \qquad [3]$$

The Levenberg-Marquardt iterative algorithm was also used to gradually approximate the original data, the obtained fitting curves were shown in Figure 12, and the corresponding fitting functions were shown in Table 6.

From Figure 9, it could be seen that the particle size range of the sand had a significant influence on the shear strength of the concrete-sand contact surface. With an increase in particle size, the shear strength of the concrete-sand contact surface also increased. A non-linear relationship between particle size range and shear strength was observed. When the median particle size was increased from 0.22mm to 1.0mm, the average increase in shear strength was 23.7% at P=50kPa, 16.7% at P=100kPa, 22.0% at P=200kPa and 16.1% at P=300kPa. When the median particle size was increased from 1.0mm to 3.47mm, the average increase in shear strength was 10.4% at P=50kPa, 11.9% at P=100kPa, 17.5% at P=200kPa, and 9.7% at P=300kPa. When the median particle size was increased from 0.22mm to 3.47mm, the shear strength was increased by a maximum of 43.2%. It was observed that there was a critical value for the effect of particle size on shear strength. By studying the functional relationship, it was found that the upper limit of the critical value of the particle size in this study was close to 2.0mm, and the lower limit was close to 0.5mm. The effect of the change in particle size on shear strength was weakened when it exceeded this critical range.

Similarly, from the Figure 10, it could be seen that the number of grooves also had a significant effect on the interfacial shear strength, and the shear strength rose with the increase in the number of grooves. Under lower normal stress conditions (e.g., P = 50 kPa), the interfacial shear strength was close to linear with the number of grooves, whereas the interfacial shear strength showed a nonlinear relationship with the number of grooves when the normal stress rose, and the fitted functional relationships were shown in Table 6. When the number of grooves increased from 5 to 9, the average increase in shear strength was 10.7% at P=50kPa, 24.2% at P=100kPa, 21.7% at P=200kPa and 15.0% at P=300kPa.When the number of grooves increased from 9 to 13, the average increase in shear strength was 7.3% at P=50kPa, 4.1% at P=100kPa, 5.0% at P=200kPa and 2.7% at P=300kPa. When the number of grooves was increased from 5 to 13, the shear strength was increased by a maximum of 29.3%. It was observed that there was a critical value for the impact of the number of grooves on shear strength. Studying the functional relationship, it was found that the critical value of the number of grooves in this study was close to 9. Beyond this value, the change in the number of grooves had a weakened effect on shear strength. Additionally, when the normal stress was 100-200kPa, the change in the number of grooves had the highest efficiency in improving shear strength.

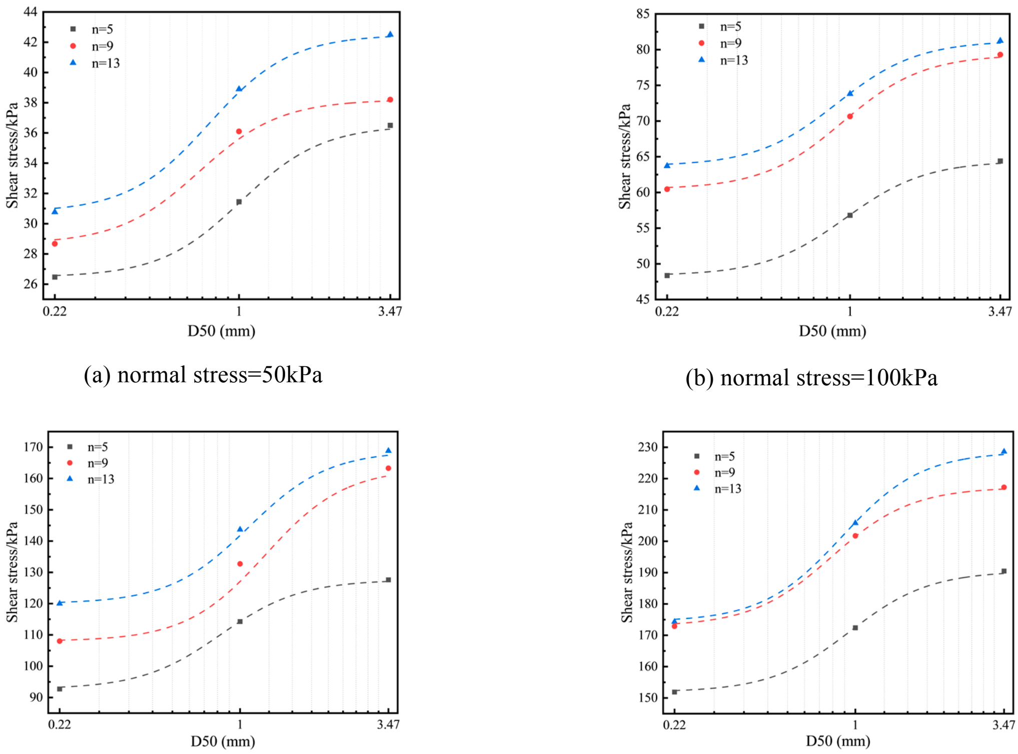

(a) normal stress=50kPa

(b) normal stress=100kPa

(c) normal stress=200kPa

(d) normal stress=300kPa

FIGURE 11. Fitted shear strenght curves under different sand particles size ranges.

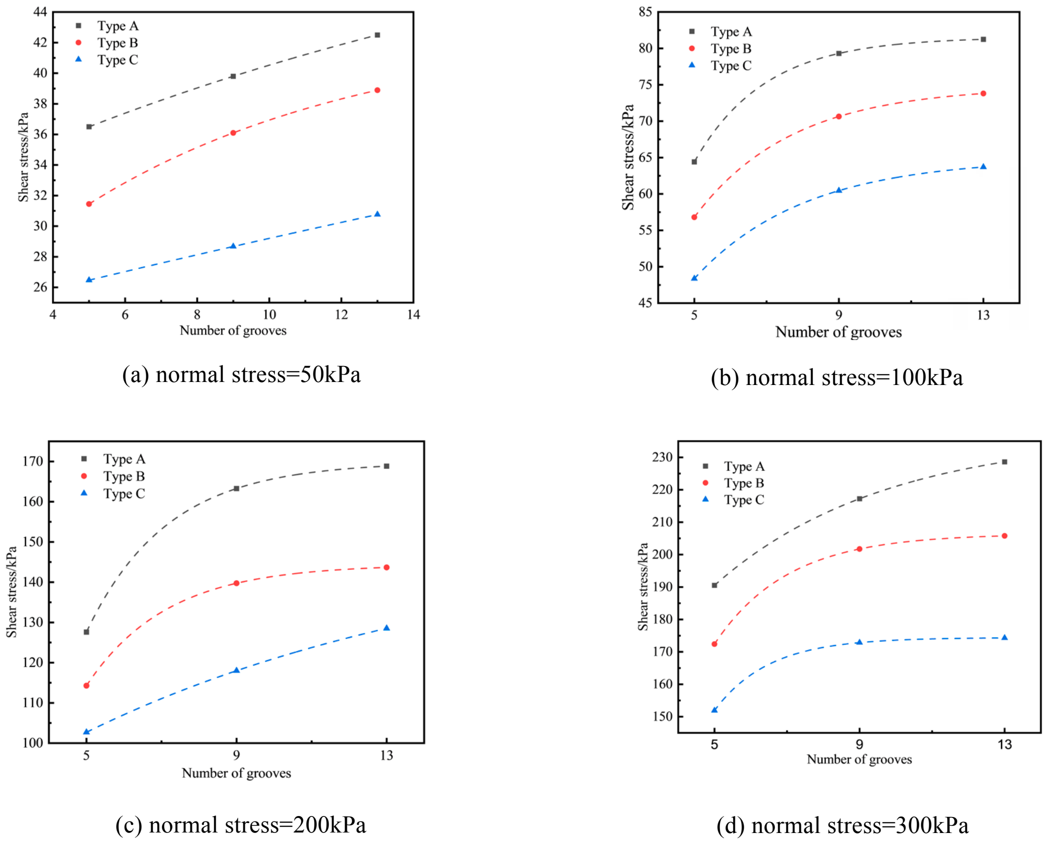

(a) normal stress=50kPa

(b) normal stress=100kPa

(c) normal stress=200kPa

(d) normal stress=300kPa

Figure 12. Fitted shear strength curves under different groove numbers..

Table 6. Fitted equations between shear strength and median particle size (D50) and number of grooves.

Serial number	functional relationship	Particle size range（mm）	Curve equation	R^2
1	y: shear strength x: D50	Type A sand	$y = 101.6 + 67(1 - e^{-x/4.6}) + 67.7(1 - e^{-x/4.6})$	1
		Type B sand	$y = -198.9 + 202.7(1 - e^{-x/2.0}) + 202.67(1 - e^{-x/2.0})$	1
		Type C sand	$y = -464.8 + 319.6(1 - e^{-x/1.49}) + 319.6(1 - e^{-x/1.49})$	1
2	y: shear strength x: groove number	Type A sand	$y = \frac{-38.6}{1 + (x/0.95)^3} + 190.5$	0.999
		Type B sand	$y = \frac{-44.4}{1 + (x/0.82)^3} + 217.2$	0.999
		Type C sand	$y = \frac{-54.3}{1 + (x/0.89)^3} + 228.6$	0.999

According to the fitting equations for shear strength in Table 5, the interfacial friction angle of various types of sand under the condition of different number of grooves was determined, and the relationship between it and the type of sand was drawn as shown in Figure 11. Figure 13 visually reflected the relationship between the internal friction angle and the particle size range of sand, it indicated that the larger the particle size range, the larger the interfacial friction angle. When the number of grooves was 5, the friction angle of the Class A sand-concrete interface was 111.00% of the Class B sand-concrete interface and 124.11% of the Class C sand-concrete interface. When the number of grooves was 9, the friction angle of the Class A sand-concrete interface was 110.65% of the Class B sand-concrete interface and 130.29% of the Class C sand-concrete interface. When the number of grooves was 13, the friction angle of the Class A sand-concrete interface was 112.93% of the Class B sand-concrete interface and 131.58% of the Class C sand-concrete interface. Under the same roughness, it could be seen that the greater the number of grooves, the greater the internal friction angle of the contact surface. However, the internal friction angles measured under different shear conditions were smaller than that of pure sand.

4. NUMERICAL MODELING AND ANALYSIS

4.1. The establishment of PFC model and the determination of parameters

During the shear process, the particles near the interface moved due to the dislocation between the upper and lower shear boxes. Rotational motion was a direct result of shear stress, the rotation angle of the particles could indicate the strength of the particles subjected to shear, and the distribution range of the rotating particles could indicate the distribution range of the interfacial shear band. It was still not able to capture the particle rotation characteristics accurately and intuitively under indoor test conditions. Therefore, this study utilized PFC2D 6.0 software to establish a discrete element analysis model with the same size as the sample in the indoor test according to the shear test conditions. In the modelling process, the typical particle morphology in the sand specimen was selected, and then the CAD software was used to depict the 2D profiles of the typical particles and save the outlines as DXF files. The profiles of 7 types of typical particle were shown in Figure 14, and the maximal profile diameter of each particle was approximated to be equal. The PFC software was used to import DXF files to identify and generate templates. Each template was then filled with a number of circular particles. The ratio of the maximum circular particle diameter to the minimum circular particle diameter in each template was set to 0.1, and the proportion of circular particles exceeding the template boundary was set to 5%. The resulting rigid cluster particle template formed after particle filling was shown in Figure 15. In the process of generating the sand model, the particle sizes of each template were multiplied in order by the amplification coefficient designed in equal proportions. This ensured that the minimum and maximum particle sizes generated conformed to the maximum and minimum particle sizes in the gradation curve. Additionally, the particle sizes of other templates were distributed in the particle size range according to the principle of equal proportion. Finally, the same mass fraction as the gradation curve was generated according to the template order. Unfortunately, the current sand model did not fully reflect the true mass fractions of different shapes of sand particles, as a detailed classification of the shapes of sand particles had not been carried out along with an investigation of the mass fractions of the different shapes.

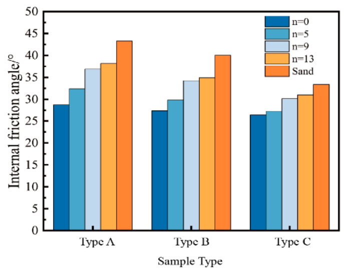

Figure 13. The relationship between the internal friction angle of the contact surface and the grain size range of sand.

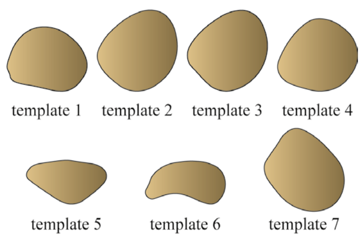

Figure 14. 7 types of typical particle profiles.

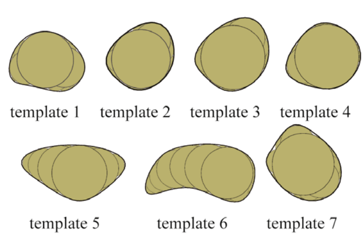

Figure 15. Clump templates filled with circular particles.

The upper and lower shear boxes and shear surfaces of the model were simulated through “generalized walls”, as shown in Figure 16(a), and the size of the model was 96mm×4.0mm (length × height). No.①②③ was the upper shear box, No.④⑥ was the blocking structure, No.⑦⑧⑨ was the lower shear box, and No.⑤ was the shear surface with semicircular grooves. During the shearing process, No.①②③⑥ were fixed, No.④⑤⑦⑧⑨ moved to the right at a speed of 1.2mm/min, and the maximum shearing displacement was set to 7mm. The normal and tangential contact stiffness between particles was set to 2×108 N/m, the normal and tangential contact stiffness between particles and walls was also set to 2×108 N/m, the normal pressure was set to 300 kPa, the interfacial friction coefficient was set to 0.32, and the interparticle friction coefficient was set to 0.91. Figure 16(a), (b), and (c) represented shear models corresponding to type A sand samples, type B sand samples, and type C sand samples respectively. To increase the continuity of the change in the number of grooves, two working conditions with the number of grooves n=7 and n=11 were added to the numerical model, and the geometrical characteristics of the grooves of the added interfaces were shown in Table 7. Finally, a total of five types of semicircular shear interfaces with the same roughness (n=5/7/9/11/13) were designed into the numerical model.

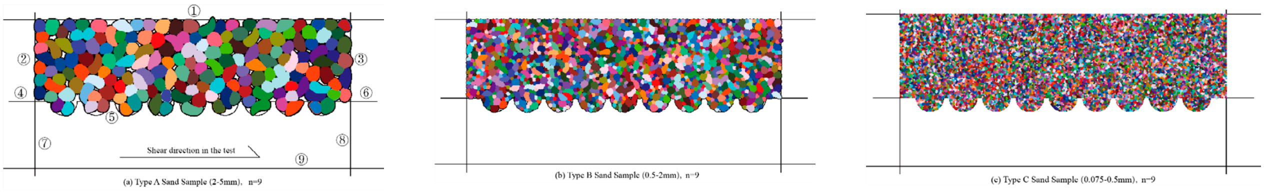

Figure 16. Numerical model of direct shear for serrated contact surfaces (n=9).

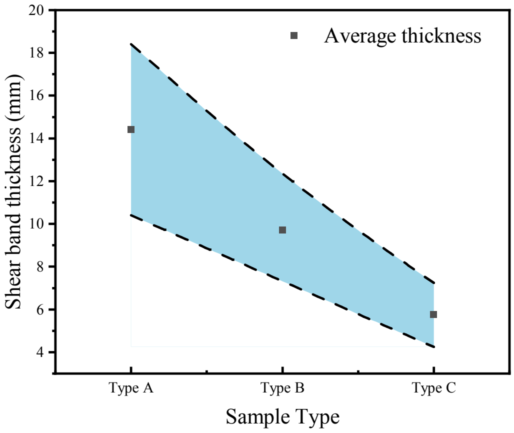

Figure 17. Shear band thickness of Type A, B and C sand under direct shear test.

Table 7. Design parameters of concrete test blocks with different numbers of grooves.

Concrete test block	L (mm)	H (mm)	l_1 (mm)	l_2 (mm)	l_3 (mm)	h_1 (mm)
n=7	96	20	9.1	3.1	6.5	4.6
n=11	96	20	7.5	0.5	4.25	3.6

4.2. Analysis of numerical simulation results

The accuracy of numerical simulation results is closely related to the input parameters. Regrettably, it is unable to acquire particle parameters such as contact stiffness, interparticle friction angle, and particle elastic modulus at the microscopic level through laboratory experiments in this study. As an alternative, the relevant microscopic parameters were determined by reviewing references and using analogy methods. While the shear curves obtained through numerical simulation may not perfectly reflect the actual shear process, its reliability was high regarding particle motion laws and interparticle interaction mechanisms. Therefore, the shear displacement curves obtained through numerical simulation were not presented but instead explored the results of the numerical simulation in the perspective of shear mechanisms.

It shows that increasing the particle size can not only improve the interfacial shear strength, but also increase the thickness of the shear zone (14, 16 40, 41). From Figure 17, it can be seen that the influence of the particle size range on the interfacial shear characteristics is as follows: (1) the shear band thickness increases rapidly with the increase of particle size, and the fluctuation range of the shear band thickness in different particle size ranges also increases. Specifically, the shear band thickness of Type A sand is 12.4-16.4mm, the shear band thickness of Type B sand was 8.5-10.92mm, and the shear band thickness of Type C sand is 5.0-6.5mm. （2）The boundaries of the shear bands generated in Type B sand and Type C sand are clear, while the boundaries of the shear bands of Type A sand are blurred. Presumably due to the influence of the particle size effect, the matching degree between the particle diameter and the size of the shear box is reduced.

During the shearing process, the upper sand particles underwent rotation and translation movements, and the movement rules were closely related to factors such as the position of the sand particles, the amount of shear displacement, and the geometric characteristics of the interface. Particle rotation was primarily caused by shear action at the interface, so these rotation characteristics could directly reflect the development characteristics of the shear band within the interface range. Therefore, in this study, the angle of particle rotation was used as an analytical variable to analyze the influence of particle size range on the development laws of the shear band under different numbers of semicircular grooves. To conserve pages, the state at a shear displacement of 3 mm was taken as the analysis object, and the rotation angle of the particles at the beginning of the shear test was 0°. During the numerical test, the monitoring function of PFC was used to record the particle rotation angle, and after the numerical test was completed, the data such as the particle position and the cumulative particle rotation angle in the result file were exported to TXT data text by using the compilation function of the FISH language in the PFC software. The data text was imported into OriginPro 2024 (64-bit) SR1 software, and the cloud diagrams were drawn using the plotting function of the software, with the diameter of the specimen as the X-coordinate and the height of the specimen as the Y-coordinate. The 'surface' splatter was used to fill in the color of the cloud diagrams, which had 20 gradients, in order to increase the contrast of the cloud diagrams, the gradient of the cloud diagram was displayed in non-linear type 'probit', so that it was easy to analyse the distribution pattern of the shear bands. Since there was no rotation and corresponding particle information in the lower part of the groove model, the boundary lines of the groove model were plotted by using Auto CAD software and exporting the geometric information of the boundary lines as TXT text. After modifying the format, the text data were imported into OriginPro 2024 (64-bit) SR1 software, and a column of data with particle rotation angle of 0 was added for plotting within the specified analysis range. Finally, the two plots completed before and after were superimposed to obtain the distribution cloud diagrams shown in Figure 18 to Figure 20.

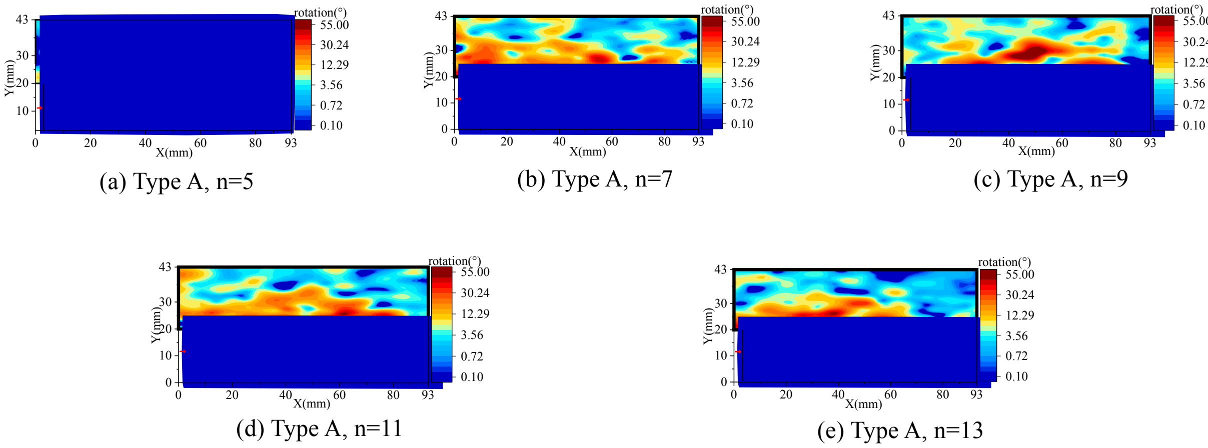

Figure 18. Cloud diagram of particle rotation angles of Type A sandy soil under different numbers of grooves.

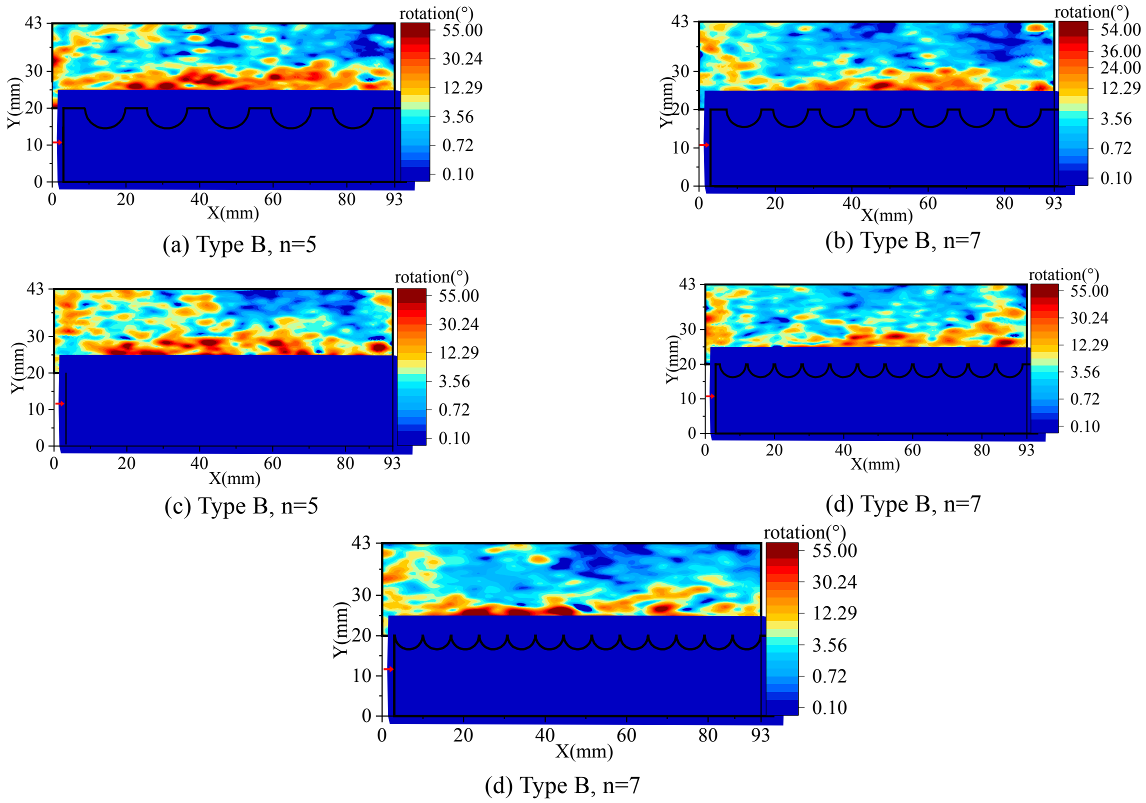

Figure 19. Cloud diagram of particle rotation angles of Type B sandy soil under different numbers of grooves.

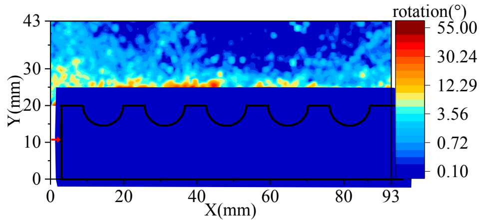

(a) Type C, n=5

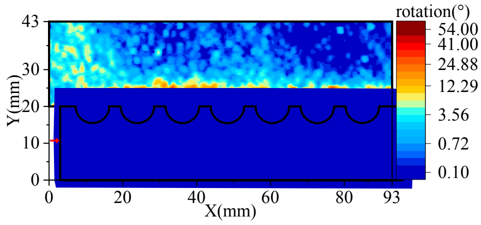

(b) Type C, n=7

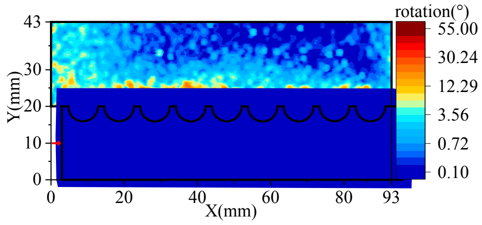

(c) Type C, n=9

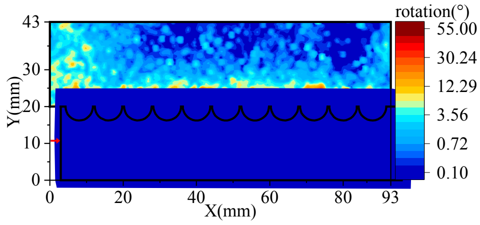

(d) Type C, n=11

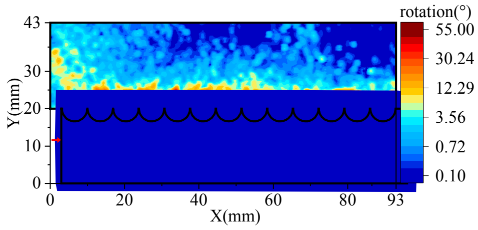

(e) Type C, n=13

Figure 20. Cloud diagram of particle rotation angles of Type Csandy soil under different numbers of grooves.

The thickness of the shear band increases with surface roughness (30), while changes in the number of grooves in this study do not affect surface roughness. The influence of the grooves number on shear characteristics is as follows: (1) Increasing the number of grooves do not result in a significant increase in the thickness of the shear band, and the degree of particle rotation do not change regularly.(2) The distribution of particle rotation at both ends of the upper shear box is closely related to the shear direction. When the shear direction is from left to right, there are significantly more particles rotating at the left end of the upper shear box compared to the right end. This occurs because, after shear displacement, the gap between the particles at the left end increases, leading to a higher probability of particle rotation. Conversely, the right end is compressed, resulting in a reduced gap and a decreased probability of particle rotation.

Overall, the rotation angle of the particles increases along the depth of the contact surface, with the maximum rotation angle occurring near the contact surface. The areas where intense rotation occurred are primarily distributed at the top edge of the groove surface. It can be seen that the sand particles at the upper corner of the groove have greater amplitudes of sliding and rotation. The resistance between these sand particles is consequently higher, resulting in greater shear stress being generated in this area. With an increase in the number of grooves on the concrete slab, there is a corresponding increase in the number of sand particles that rotate at the interface, leading to more frequent interactions between the sand particles and consequently resulting in higher interface shear strength. As the particle size of the sand decreases, there is a transition in the rotation angle distribution of sand particles from discrete to continuous along the cross-section. It leads to clearer boundaries between the rotation angles of the sand particles, particularly evident at the upper edge of the groove, where there is an overall decrease in the values of rotation angle. The reason behind this phenomenon is that smaller sand particles have weaker resistance against the edges of grooves. Consequently, the force required to counteract bite force, rolling friction, and sliding friction decreases. It results in smoother and more uniform force characteristics at the interface. Comparing the results of numerical simulation with the results of indoor shear experimental, it is found that the shear mechanical properties demonstrated by both sets of results are fundamentally consistent.

5. ANALYSIS OF SHEAR MECHANISM

After the direct shear test, the contact situation of the interface between sand in different particle size ranges and the concrete surface with grooves can be intuitively observed by photographing the contact surfaces, as shown in Figure 21. Distribution characteristics of interfacial particles in each working condition after direct shear test., where the letters represent the types of sand and the numbers represent the number of grooves.

In the case of the same number of grooves, the larger the particle size of the sand, the larger the contact area between a single sand particle and the groove surface, resulting in greater resistance to the groove surface. On the contrary, the smaller the size of the sand particles, the greater the number of sand particles that can be filled in a single groove, the smaller the friction and bite force between the sand grains and the groove surface, and between the sand particles and sand particles, resulting in the less shear force required for friction, flip, and dislocation of particles.

The number of grooves on the contact surface also affects the interaction between the sand particles and the concrete slab. During the direct shear test, under the conditions of same sand sample, increasing the number of grooves results in more interfacial edges and corners, leading to greater shear stress generated by the resistance between sand particles and concrete. Consequently, under a certain surface roughness, the shear strength increases as the number of grooves increases.

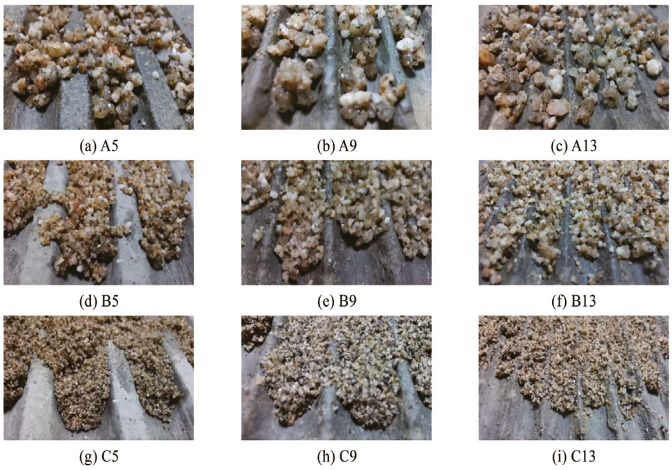

Figure 21. Distribution characteristics of interfacial particles in each working condition after direct shear test.

The number of grooves on the contact surface also affects the interaction between the sand particles and the concrete slab. During the direct shear test, under the conditions of same sand sample, increasing the number of grooves results in more interfacial edges and corners, leading to greater shear stress generated by the resistance between sand particles and concrete. Consequently, under a certain surface roughness, the shear strength increases as the number of grooves increases.

The increase in normal stress during direct shear is also an important factor affecting the shear strength of the concrete-sand contact surface. As the normal stress increases, the bond between sand and concrete is strengthened, leading to greater bite force generated at the interface. It results in sand particles fitting more closely into the grooves, leading to increased friction force and higher shear strength. Additionally, as the particle size of the sand increases, the changes in interfacial shear mechanical properties becomes more obvious.

6. DISCUSSION

6.1. Relationship between shear strength and number of grooves

In this study, it was found that the spacing density of the semicircular groove in contact surface had a significant effect on the shear strength of the interface under the same roughness, the shear strength of the contact surface could be improved by 29.3% under the optimal conditions, the shear strength was nonlinearly related to the groove density, and the functional relationship was in accordance with the ExpAssoc function characteristic. The fitting results indicated that the change in shear strength was most sensitive when the number of grooves was between 5 and 9,with the spacing of grooves varing from 5.9 mm to 1.67mm, the shear strength increases the fastest. When the number of grooves was greater than 9, the sensitivity to changes in shear strength decreased, probably due to saturation of the action between the grooves. The study confirmed the hypothesis that the degree of excitation of interfacial shear strength is closely related to the geometric properties and spatial distribution of interfacial texture (20,21). The findings of this research have significant implications for the design and construction of a range of practical projects, including retaining walls, pile foundations, and underground structures, and the engineer can choose the appropriate design scheme for the contact surface based on the characteristics of the sand materials on different sites.

6.2. Influence of sand particle size on shear strength

The study had also found that particle size had a significant effect on shear strength, verifying the phenomenon of strong positive correlation between peak shear strength of the contact surface and changes in content of the coarse particles and particle size ratio (16). In this study, the direct shear test on the contact surface of sand with three different particle size ranges (2~5mm, 0.5~2mm, 0.075~0.5mm) and concrete revealed that the particle size of sand had a significant effect on the shear strength under the same roughness of the contact surface, and the shear strength could be improved by 43.2% when the median particle size was increased from 0.22mm to 3.47mm. Analysis of the fitted function curves revealed that the efficiency of improving the shear strength was highest when the median particle size of the sand samples varied between 0.5 mm and 2.0 mm, beyond which the effect of particle size on shear strength diminished.

6.3. Changes in the thickness of the shear band

The thickness of the shear band at the contact surface is generally not directly observable. In this study, numerical simulation was used to investigate the change of the thickness of the shear band. The results of numerical simulation indicated that the thickness of the shear band increased rapidly with the increase of particle size, and the fluctuation range of thickness of the shear band in different particle size ranges also increased. Among them, the thickness of the shear band in Type A sand ranged from 12.4mm to16.4 mm, the thickness of the shear band in Type B sand ranged from 8.5mm to 10.92 mm, and the thickness of the shear band in Type C sand ranged from 5.0mm to 6.5 mm. The increase in the number of grooves did not lead to a significant increase in the thickness of the shear band.

6.4. Changes in particle scale and motion characteristics

The particle motion characteristics in the shear process are generally not directly observable. This study combined the distribution characteristics of the particles on the contact surface at the end of the shear test and the motion characteristics of the particles in the shear process of the numerical simulation and found that as the range of particle sizes varied from large to small, the sand particles change from violent staggering and overturning to low-intensity inter-particle sliding friction as they pass through the grooves, corresponding to a similar reduction in the resulting shear strength and a similar reduction in the strain softening effect.

7. CONCLUSIONS

In this paper, the shear mechanical properties of sand with different particle sizes on the surface of concrete slabs with different grooves were investigated under certain roughness. After systematic work such as indoor direct shear tests and numerical analysis, the conclusions are as follows:

(1) In this study, it is found that the density of grooves significantly affects the shear strength of the interface under the condition of same roughness, and the shear strength can be increased by 29.3% under the optimum condition. However, this effect decreases with the increase of the number of grooves, especially when the number of grooves exceeds 9.

(2) The sand particle size has a significant effect on the shear strength of the interface, and the shear strength can be increased by 43.2% when the median grain size increases from 0.22mm to 3.47mm. The efficiency of improving shear strength was most significant when the sand particle size ranges from 0.5mm to 2.0mm.

(3) The results of the numerical simulations shows that the increase in particle size leds to an increase in the thickness of the shear band, but the increase in the number of grooves do not significantly change the thickness of the shear band.

(4) Changes in the motion characteristics of the particles reveal a transition from staggering to intergranular sliding. This finding provides a new perspective for understanding the reduction of shear strength.

Funding Sources

Research carried out within the framework of Grant No. 2022A-231-G, financed by the Yongjiang Talent Project, and grant No. Y202249605, financed by the General Scientific Research Projects of Zhejiang Education Department.

Authorship contribution statement

Zhigang Meng: Conceptualization, Formal analysis, Fund raising, Research, Methodology, Software, Visualization, Write-up - original draft, Write-up - review & editing.
Yunsong Li: Data cleansing, Formal analysis, Software, Validation, Write-up - original draft.
Huanhuan Li: Conceptualization, Research, Methodology, Project administration, Supervision, Write-up - review & editing.
Jiyuan Xu: Data cleansing, Formal analysis, Validation.
Songlin Shen: Data cleansing, Formal analysis, Research, Write-up - original draft.

Declaration of competing interest

The authors of this article declare that they have no financial, professional or personal conflicts of in-terest that could have inappropriately influenced this work.

REFERENCES

1. Afzali-Nejad A, Lashkari A, Shourijeh PT. 2017. Influence of particle shape on the shear strength and dilation of sand-woven geotextile interfaces. Geotext. Geomembr. 45(1):54-66. https://doi.org/10.1016/j.geotexmem.2016.07.005

2. Athanasopoulos GA. 1993. Effect of particle size on the mechanical behaviour of sand-geotextile composites. Geotext. Geomembr. 12(3):255–273. https://doi.org/10.1016/0266-1144(93)90029-n

3. O'Rourke TD, Druschel SJ, Netravali AN. 1990. Shear strength characteristics of sand-polymer interfaces. J. Geotech. Eng. 116(3):451–469. https://doi.org/10.1061/(asce)0733-9410(1990)116:3(451)

4. Bhandari A, Han J, Parsons RL. 2010. DEM analysis of geotextile-soil interaction under wheel loading. Research Symposium on Characterization and Behavior of Interfaces. 99-106. https://doi.org/10.3233/978-1-60750-491-7-99

5. Göktepe AB, Sezer A. 2010. Effect of particle shape on density and permeability of sands. Proceedings of the Institution of Civil Engineers - Geotechnical Engineering. 163(6):307–320. https://doi.org/10.1680/geng.2010.163.6.307

6. Liu F, Ying M, Yuan G, Wang J, Gao Z, Ni J. 2021. Particle shape effects on the cyclic shear behaviour of the soil–geogrid interface. Geotext. Geomembr. 49(4):991–1003. https://doi.org/10.1016/j.geotexmem.2021.01.008

7. Nakata Y, Hyde AFL, Hyodo M, Murata H. 1999. A probabilistic approach to sand particle crushing in the triaxial test. Geotech. 49(5):567–583. https://doi.org/10.1680/geot.1999.49.5.567

8. Su L, Zhou W, Chen W, Jie X. 2018. Effects of relative roughness and mean particle size on the shear strength of sand-steel interface. Measurement. 122:339–346. https://doi.org/10.1016/j.measurement.2018.03.003

9. Wang H, Zhang Q, Yin Z, Jing H. 2023. Effect of sand particle size on interface shear behaviour between bio-cemented sand by MICP treatment and steel structure. Can. Geotech. J. 60(3):269–286. https://doi.org/10.1139/cgj-2021-0387

10. Wang J, Ying M, Liu F, Yuan G, Fu H. 2021. Experimental investigation on the stress-dilatancy response of aggregate-geogrid interface using parameterized shapes. Constr. Build. Mater. 289:123170. https://doi.org/10.1016/j.conbuildmat.2021.123170

11. Gayathri VL, Vangla P, Riya A. 2022. Effect of snakeskin-inspired patterns on the shear response of soil - continuum interfaces. Int. J. Geotech. Eng. 16(6):759–775. https://doi.org/10.1080/19386362.2022.2066049

12. Namjoo AM, Jafari K, Toufigh V. 2020. Effect of particle size of sand and surface properties of reinforcement on sand-geosynthetics and sand–carbon fiber polymer interface shear behavior. Transp. Geotech. 24:100403. https://doi.org/10.1016/j.trgeo.2020.100403

13. Rousé PC, Fannin RJ, Shuttle DA. 2008. Influence of roundness on the void ratio and strength of uniform sand. Géotechnique. 58(3):227–231. https://doi.org/10.1680/geot.2008.58.3.227

14. Vangla P, Latha GM. 2016. Effect of particle size of sand and surface asperities of reinforcement on their interface shear behaviour. Geotext. Geomembr. 44(3):254–268. https://doi.org/10.1016/j.geotexmem.2015.11.002

15. Lopes MJ, Lopes ML. 1999. Soil-geosynthetic interaction - influence of soil particle size and geosynthetic structure. Geosynth. Int. 6(4):261–282. https://doi.org/10.1680/gein.6.0153

16. Vangla P, Latha GM. 2015. Influence of particle size on the friction and interfacial shear strength of sands of similar morphology. Int. J. Geosynth. Ground Eng. 1:6. https://doi.org/10.1007/s40891-014-0008-9

17. Rasti A, Adarmanabadi HR, Pineda MC, Reinikainen J. 2021. Evaluating the effect of soil particle characterization on internal friction angle. Am. J. Eng. Appl. Sci. 14(1):129–138. https://doi.org/10.3844/ajeassp.2021.129.138

18. Taiba AC, Mahmoudi Y, Azaiez H, Belkhatir M. 2023. Impact of the overall regularity and related granulometric characteristics on the critical state soil mechanics of natural sands: a state-of-the-art review. Geomech. Geoeng. 18(4):299–308. https://doi.org/10.1080/17486025.2022.2044076

19. Cho GC, Dodds J, Santamarina JC. 2006. Particle shape effects on packing density, stiffness, and strength: natural and crushed sands. J. Geotech. Geoenviron. Eng. 132(5):591-602. https://doi.org/10.1061/(asce)1090-0241(2006)132:5(591)

20. Frost JD, Karademir T. 2016. Shear-induced changes in smooth geomembrane surface topography at different ambient temperatures. Geosynth. Int. 23(2):113-128. https://doi.org/10.1680/jgein.15.00036

21. Subaida EA, Chandrakaran S, Sankar N. 2008. Experimental investigations on tensile and pullout behaviour of woven coir geotextiles. Geotext. Geomembr. 26(5):384–392. https://doi.org/10.1016/j.geotexmem.2008.02.005

22. Anubhav, Basudhar PK. 2013. Interface behavior of woven geotextile with rounded and angular particle sand. J. Mater. Civ. Eng. 25(12):1970–1974. https://doi.org/10.1061/(asce)mt.1943-5533.0000774

23. Deiminiat A, Li L, Zeng F. 2022. Experimental study on the minimum required specimen width to maximum particle size ratio in direct shear tests. Civ. Eng. 3(1):66–84. https://doi.org/10.3390/civileng3010005

24. Liu F, Zheng Q, Wang J, Fu H, Gao Z, Ni J. 2022. Effect of particle shape on shear behaviour of aggregate-geogrid interface under different aperture ratios. Int. J. Pavement Eng. 23(7):2099–2109. https://doi.org/10.1080/10298436.2020.1843035

25. Liu S, Zhang Q, Ma B, Li Z, Yin W, Lou Q. 2023. Study on surface roughness effect on shear behavior of concrete-soil interface. Eng. Fail. Anal. 145:107050. https://doi.org/10.1016/j.engfailanal.2023.107050

26. Wang R, Ong, DEL, Peerun MI, Jeng DS. 2022. Influence of surface roughness and particle characteristics on soil–structure interactions: a state-of-the-art review. Geosciences. 12(4):145. https://doi.org/10.3390/geosciences12040145

27. Ying M, Liu F, Wang J, Wang C, Li M. 2021. Coupling effects of particle shape and cyclic shear history on shear properties of coarse-grained soil–geogrid interface. Transp. Geotech. 27:100504. https://doi.org/10.1016/j.trgeo.2020.100504

28. Cavarretta I, Coop M, O'Sullivan C. 2010. The influence of particle characteristics on the behaviour of coarse grained soils. Géotechnique. 60(6):413-423. https://doi.org/10.1680/geot.2010.60.6.413

29. Dai B, Yang J, Zhou C. 2016. Observed effects of interparticle friction and particle size on shear behavior of granular materials. Int. J. Geomech. 16(1):04015011. https://doi.org/10.1061/(asce)gm.1943-5622.0000520

30. DeJong JT, Westgate ZJ. 2009. Role of initial state, material properties, and confinement condition on local and global soil-structure interface behavior. J. Geotech. Geoenviron. Eng.135(11):1646-1660. https://doi.org/10.1061/(asce)1090-0241(2009)135:11(1646)

31. Coetzee CJ. 2016. Calibration of the discrete element method and the effect of particle shape. Powder Technol. 297,50-70. https://doi.org/10.1016/j.powtec.2016.04.003

32. Ferellec JF, McDowell GR. 2012. Modelling of ballast–geogrid interaction using the discrete-element method. Geosynth. Int. 19(6):470-479. https://doi.org/10.1680/gein.12.00031

33. Gao G, Meguid MA. 2018. Effect of particle shape on the response of geogrid-reinforced systems: Insights from 3D discrete element analysis. Geotext. Geomembr. 46(6):685–698. https://doi.org/10.1016/j.geotexmem.2018.07.001

34. Khanal M, Elmouttie M, Adhikary D. 2017. Effects of particle shapes to achieve angle of repose and force displacement behaviour on granular assembly. Adv. Powder Technol. 28(8):1972–1976. https://doi.org/10.1016/j.apt.2017.04.016

35. Wang Z, Jacobs F, Ziegler M. 2016. Experimental and DEM investigation of geogrid–soil interaction under pullout loads. Geotext. Geomembr. 44(3):230–246. https://doi.org/10.1016/j.geotexmem.2015.11.001

36. Xu J, Liu J, Shi X, Ji F, Zeng Y. 2024. DEM investigation of the effect of coarse content and size ratio on the local shear behavior at gap-graded soil-structure interface. Powder Technol. 433:119281. https://doi.org/10.1016/j.powtec.2023.119281

37. Anubhav, Wu H. 2015. Modelling of non-linear shear displacement behaviour of soil–geotextile interface. Int. J. Geosynth. Ground Eng. 1:19. https://doi.org/10.1007/s40891-015-0021-7

38. Paulick M, Morgeneyer M, Kwade A. 2015. A new method for the determination of particle contact stiffness. Granular Matter. 17:83–93. https://doi.org/10.1007/s10035-014-0537-x

39. Li H, Fu S, Zhu D, Li G, Shen S. 2023. Experimental study on the effects of triangular groove inclination angles on the mechanical behavior of sand–concrete interfaces. J. Mater. Res. Technol. 24:159–172. https://doi.org/10.1016/j.jmrt.2023.02.208

40. Jing X, Zhou W, Zhu W, Zhu H, Yin Z, Li Y. 2018. Analysis of soil-structural interface behavior using three-dimensional DEM simulations. Int. J. Numer. Anal. Methods Geomech. 42(2):339-357. https://doi.org/10.1002/nag.2745

41. Wang J, Gutierrez MS, Dove JE. 2007. Numerical studies of shear banding in interface shear tests using a new strain calculation method. Int. J. Numer. Anal. Methods Geomech. 31(12):1349-1366. https://doi.org/10.1002/nag.589